THE ASTRONOMICAL JOURNAL, 121:140–147, 2001 January
© 2001. The American Astronomical Society. All rights reserved. Printed in U.S.A.

A BROAD SEARCH FOR COUNTERROTATING GAS AND STARS: EVIDENCE FOR MERGERS AND ACCRETION

S. J. KANNAPPAN AND D. G. FABRICANT
Harvard-Smithsonian Center for Astrophysics, Mail Stop 20, 60 Garden Street, Cambridge, MA 02138; skannappan@cfa.harvard.edu, dfabricant@cfa.harvard.edu
Received 2000 July 23; accepted 2000 September 12

ABSTRACT

We measure the frequency of bulk gas-stellar counterrotation in a sample of 67 galaxies drawn from the Nearby Field Galaxy Survey, a broadly representative survey of the local galaxy population down to $M_B \sim -15$. We detect four counterrotators among 17 E/S0's with extended gas emission (24^{+8}_{-6}%). In contrast, we find no clear examples of bulk counterrotation among 38 Sa–Sbc spirals, although one Sa does show peculiar gas kinematics. This result implies that, at 95% confidence, no more than 8% of Sa–Sbc spirals are bulk counterrotators. Among types Sc and later, we identify only one possible counterrotator, a Magellanic irregular. We use these results together with the physical properties of the counterrotators to constrain possible origins for this phenomenon.

Key words: galaxies: evolution — galaxies: formation — galaxies: interactions — galaxies: kinematics and dynamics

1. INTRODUCTION

Galaxies with counterrotating gas and stars offer dramatic evidence for the hypothesis of hierarchical galaxy formation. Counterrotation highlights the possibility of multiple events in a galaxy's formation history, as opposed to isolated collapse and infall models (Rubin 1994; Schweizer 1998). Studies of elliptical, S0, and Sa galaxies have demonstrated that gas-stellar counterrotation and related phenomena such as noncoplanar rotation may be quite common (e.g., Bertola, Buson, & Zeilinger 1992; Jore 1997), although cospatial stellar-stellar counterrotation may be less so (Kuijken, Fisher, & Merrifield 1996). However, the frequency of these phenomena in the general galaxy population is uncertain. Equally important, we do not know whether the physical processes responsible for counterrotation merely perturb the host galaxy along the Hubble sequence or completely reshape it. Comparisons of gas accretion and merger scenarios have been inconclusive (Thakar et al. 1997; Galletta 1996).

Combining the compilation of Galletta (1996; review) with a few recent discoveries (Kuijken et al. 1996; Morse et al. 1998; Jore 1997), we identify in the literature at least 18 elliptical and S0 gas-stellar counterrotators, as well as nine spiral and later type galaxies. Noncoplanar rotation, particularly in the stable configuration of a polar ring, may also be common: Whitmore et al. (1990) list six kinematically confirmed polar ring galaxies and many more visual candidates. Unfortunately the statistical implications of these numbers are unclear, since so many of the discoveries were serendipitous.

To date, the best statistical estimates of the frequency of gas-stellar counterrotation come from studies restricted to early type galaxies. Bertola et al. (1992) and Kuijken et al. (1996) have analyzed samples of emission-line S0's and report that ~20%–25% of these galaxies show counterrotation or other strong kinematic decoupling between the gas and stars. Jore (1997) has surveyed 23 isolated, unbarred Sa galaxies and finds four that show clear gas-stellar counterrotation along the major axis, with the bulk of the stars rotating opposite to the bulk of the gas (see also Haynes et al. 2000).

Here we report the frequency of gas-stellar counterrotation along the major axes of 67 galaxies ranging from ellipticals to Magellanic irregulars. This work makes use of data from the recently completed Nearby Field Galaxy Survey (NFGS, Jansen et al. 2000b, 2000a; Kannappan et al. 2000), which contains imaging, spectrophotometric, and kinematic observations for ~200 galaxies drawn from the CfA 1 redshift survey (Huchra et al. 1983). Jansen et al. (2000b) designed the survey to provide a fair sampling of the local galaxy population, with as little selection bias as possible. Galaxies were chosen without preference for morphology, environment, inclination, or color, beyond that inherent in the *B*-selected and surface-brightness limited parent survey.

An important virtue of the NFGS is its inclusion of the faint galaxy population. To counteract the observational bias toward bright galaxies, Jansen et al. (2000b) selected galaxies from CfA 1 approximately in proportion to the local galaxy luminosity function (e.g., Marzke, Huchra, & Geller 1994). The resulting sample spans luminosities from $M_B \sim -23$ to -15, limited only by the decreasing CfA 1 survey volume at faint magnitudes.

2. DATA AND METHODS

All distances and magnitudes are computed with $H_0 = 75$, using a simple Hubble flow model corrected for Virgocentric infall as in Jansen et al. (2000b).

2.1. *Sample*

The sample analyzed in this paper consists of all 67 NFGS galaxies for which we have both stellar and ionized gas rotation curve data. This group includes 100% of the E/S0's with detectable ionized gas, i.e., 17 of 57 or 30% of all E/S0's. For later types, the stellar kinematic database is incomplete: gas and stellar data are available for 38 of 52 early-type Sa–Sbc spirals (73%), and 12 of 87 later type spiral and irregular galaxies (14%). Figure 1 shows the sample in the context of the NFGS, demonstrating that the 55 E–Sbc galaxies we analyze provide a fair sample of the full survey population of emission-line galaxies, whereas the 12 galaxies typed Sc and later do not.

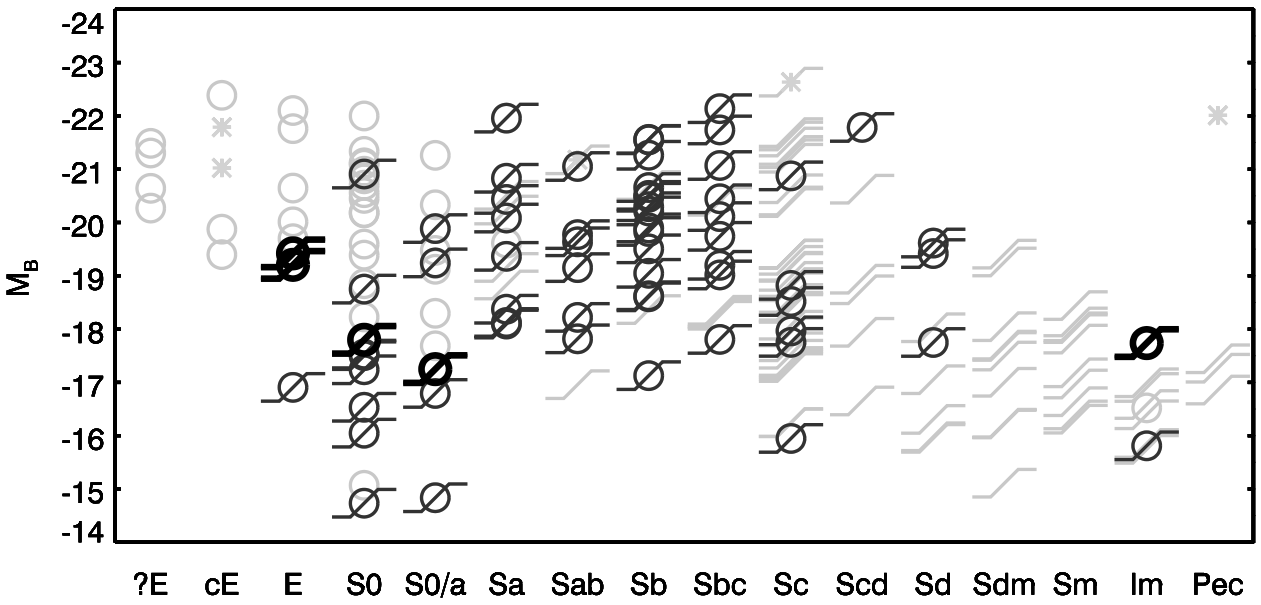

FIG. 1.—Overview of the Nearby Field Galaxy Survey, showing the demographics of all 196 galaxies sorted by morphology and *B*-band luminosity. A circular symbol indicates that we have stellar absorption-line data for the galaxy, while an S-shaped symbol indicates that we have extended gas emission-line data. The subsample of galaxies analyzed for gas-stellar counterrotation consists of all galaxies for which both symbols appear. These 67 galaxies are shaded dark gray, with counterrotators in thick black. Here we have separated S0/a's from S0's to reduce crowding in the figure, although the original morphological classification does not discriminate reliably between these two classes and all are considered "S0" in the text. A star indicates that absorption-line data were obtained but are strongly contaminated by an AGN.

2.2. *Observations and Data Reduction*

Long-slit spectra were obtained at the F. L. Whipple Observatory during several observing runs from 1996 to 1999, primarily using the FAST spectrograph on the Tillinghast Telescope (Fabricant et al. 1998). The entire data set and full details of the data reduction are described elsewhere (Kannappan et al. 2000). In most cases, we have only major axis spectra.

For the gas kinematics, we observed a 1000 Å interval centered on Hα, with a spectral resolution of $\sigma \sim 30$ km s^{-1} and a spatial binning of 2.″3 pixel^{-1}, comparable to the typical seeing of 2″. For the stellar kinematics, we observed a 2000 Å interval centered on the Mg I triplet at 5175 Å, again with 2.″3 spatial binning, but with spectral resolution $\sigma \sim 60$ km s^{-1}. We also obtained stellar kinematic data for a few galaxies with the Blue Channel Spectrograph on the MMT, using a configuration with 1.″2 binning, reduced wavelength coverage, and $\sigma \sim 40$ km s^{-1}. Spectra of nonrotating G and K giant stars were recorded to serve as velocity templates for the absorption line data.

All of the data were reduced by standard methods, including bias and dark subtraction, flat-fielding, wavelength calibration, heliocentric velocity correction, sky subtraction, spectral straightening, and cosmic-ray removal, using IRAF and IDL.

We extract high-resolution gas rotation curves (RCs) by simultaneously fitting Hα, [N II], and [S II] lines, excluding data with S/N < 3. When possible, we also derive low-resolution RCs from Hβ and [O III] lines appearing in the stellar absorption-line spectra. The low-resolution RCs act as the primary data for 10 galaxies for which we lack Hα observations and otherwise serve as confirming data. In cases of severe Hα or Hβ absorption, we rely on RCs derived from the [N II], [S II], and [O III] lines.

To extract stellar rotation curves, we cross-correlate the galaxy absorption-line spectra with the stellar template spectra in Fourier space, using xcsao in the rvsao package for IRAF (Kurtz et al. 1992). We accept fits with *R* values greater than 3.5 and error bars less than 35 km s^{-1}. We check this procedure by deriving stellar RCs with a velocity dispersion analysis code kindly provided by M. Franx, described in Franx, Illingworth, & Heckman (1989). The two methods yield consistent results within the errors. We exclude a few points in the outer parts of one galaxy, A11332+3536, where the two methods do not yield overlapping error bars.

2.3. *Identification of Gas-Stellar Counterrotators*

Operationally, we assume that a single rotation curve adequately describes the kinematics of the stars and likewise the gas. In reality, multiple velocity components may well be present (e.g., Jore 1997), but our spectra have insufficient signal-to-noise ratio for us to detect secondary velocity components in an unbiased way. Instead we search for bulk counterrotation between the gas and stars. Our approach highlights the most extreme counterrotators, but the number of counterrotators we find should be considered a lower limit.

We adopt the simplest possible definition of a counterrotator: a galaxy in which the observed gas and stellar rotation curves show opposite sign. Again, this approach yields a lower limit because our stellar curves have varying spatial extent, and some galaxies may contain undetected velocity reversals at large radii, similar to the reversal we see in NGC 3011 (Fig. 2). Furthermore, not all apparent counterrotators actually contain gas and stars in coplanar counterrotating disks. An inclined gas disk may also create an apparent counterrotation signature, and this scenario pro-

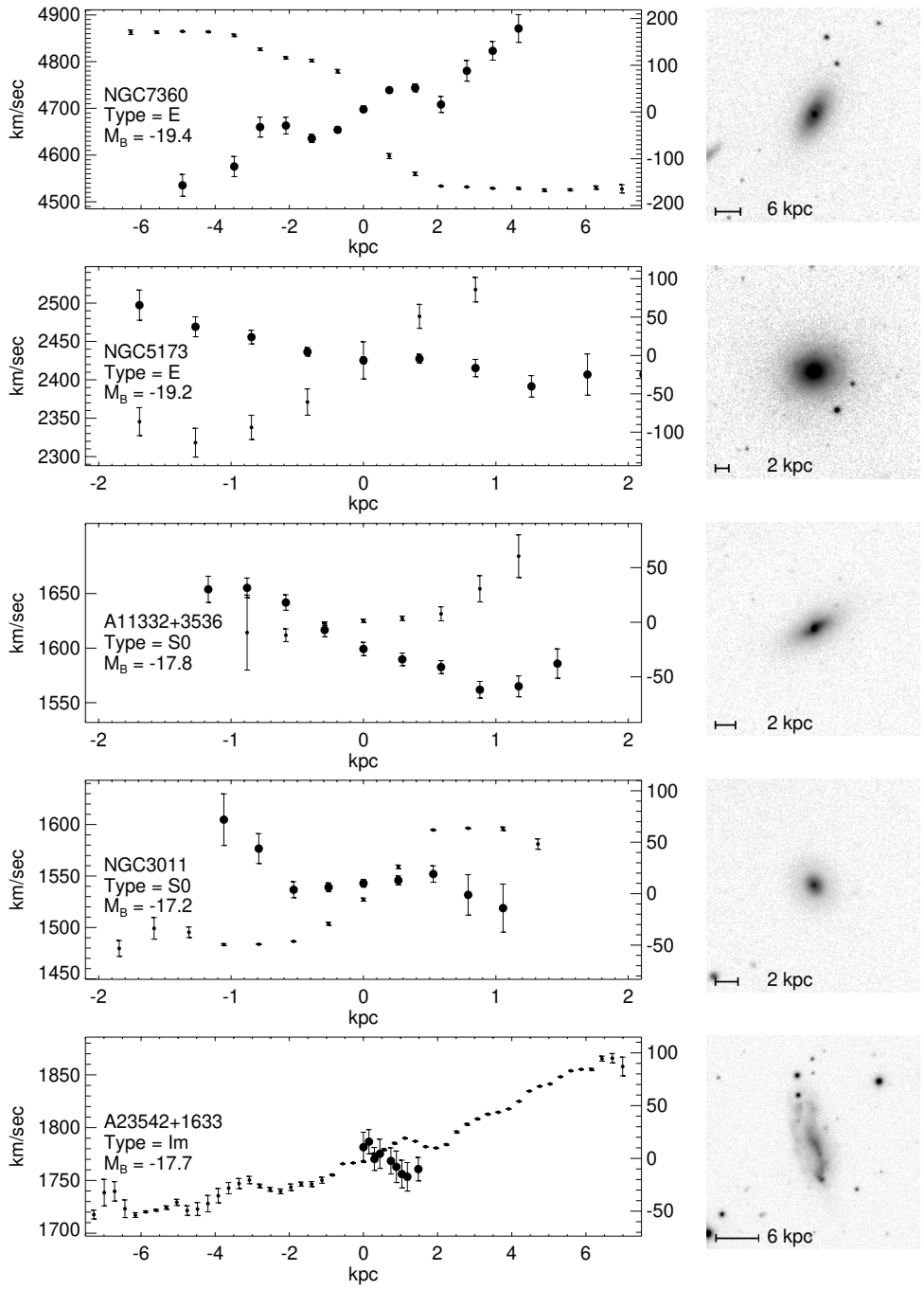

FIG. 2.—Major axis rotation curves and images for the five gas-stellar counterrotators (see Tables 1 and 2). Small dots show ionized gas emission-line data, and large dots show stellar absorption-line data. No correction has been made for inclination to the line of sight. Images shown are *U*- or *B*-band exposures, courtesy of Jansen et al. (2000b).

vides a plausible interpretation for one of our galaxies (see § 3.1). However, we note that the processes that produce inclined disks and those that produce coplanar counterrotating disks are probably similar, and the former may even evolve into the latter, so our interpretation does not rest critically on this distinction.

We estimate the confidence level for each counterrotation detection by attempting to rule out a model in which the stars simply do not rotate. Using a standard χ^2 minimization algorithm, we fit a straight line to the stellar rotation curve to determine its slope and the error on the slope. In most cases the stellar RC may be reasonably (if crudely) approximated by a straight line, except in NGC 3011, which shows a mix of corotation and counterrotation (see § 3.1). In this case we fit just the counterrotating points. The slope divided by the error on the slope constitutes the confidence level of our claim of *counter*rotation, as opposed to zero rotation. For two galaxies that we label counterrotators, the data differ from a zero rotation model by only 2–3 σ, so such a model cannot be completely ruled out. On the other

hand, three S0's and one Im galaxy rotate so little that we cannot definitely say that they are *not* counterrotators. We return to this point in § 3.2.[1]

3. RESULTS AND DISCUSSION

3.1. *Individual Counterrotators*

In our sample of 67 galaxies, we identify five likely gas-stellar counterrotators: two S0's, two Es, and 1 Im. Figure 2 shows their rotation curves and images, and Tables 1, 2, 3, and 4 summarize their properties. Figure 3 shows the available minor axis data.

We note that the type Im counterrotator found here, A23542+1633, may be the first known gas-stellar counterrotator in this morphology class, although the confidence level of the detection is not decisive (by fitting the slope as described in § 2.3, we rule out a stellar nonrotation model at 2.2 σ confidence and rule out equal-amplitude corotation at 3.2 σ confidence). Galletta (1996) lists several counterrotators as "Irr," but these are peculiar rather than Magellanic irregular galaxies. The only previous observation of any form of counterrotation in a Magellanic irregular galaxy appears to be that of Hunter et al. (1998), who have reported two counterrotating H I gas components in NGC 4449. We should of course consider the possibility that A23542+1633 might display misleading velocity reversals due to gas infall along the elongated structure on its major axis. However, the gas RC does not show large velocity reversals. The small velocity shifts near $\sim \pm 2$ kpc may reflect infall, especially given the fluctuations seen in the

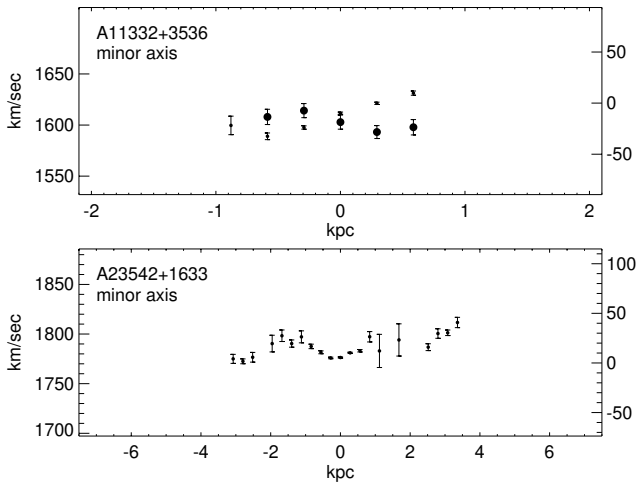

FIG. 3.—Minor axis rotation curves for A11332+3536 and A23542+1633. Small dots show ionized gas emission-line data, and large dots show stellar absorption-line data (none are available for A23542+1633). No correction has been made for inclination to the line of sight.

[1] Our sample also contains one peculiar case, an Sa galaxy (NGC 4795; see Kannappan & Fabricant 2000) in which the gas appears to be nonrotating, despite stellar velocities ~ 150 km s^{-1} and despite a tight match between the major axis position angle and the observed P.A.'s. There is a faint suggestion that better data might show counterrotation at radii $\lesssim 1$ kpc, but the present data do not permit such a claim. This is the only such case in our 67 galaxy sample. NGC 4795 exists in a field of multiple small companions, and it may be accreting one of them.

TABLE 1

BASIC PROPERTIES OF COUNTERROTATORS

Galaxy	UGC Number	Confidence[a] (σ)	Distance[b] (Mpc)	M_B[b] (mag)	r_e[b] (kpc)	Type[c]	Morphology Notes
NGC 3011.....	5259	3.0	24.0	−17.2	0.8	S0	Completely smooth
A11332+3536.....	6570	11.6	26.7	−17.8	1.2	S0	Faint inner bar+arms
NGC 5173.....	8468	5.9	38.5	−19.2	1.8	E	Outer knottiness, arms[d]
NGC 7360.....	12167	17.5	63.4	−19.4	3.9	E	Smooth, very elongated
A23542+1633.....	12856	2.2	25.4	−17.7	4.0	Im	Knotty elongated core

[a] Confidence level of claim that stars *counter*rotate, as opposed to having zero rotation. For NGC 3011, only the outer four points are considered. See § 2.3.

[b] Distances, magnitudes, and effective radii from Jansen et al. 2000b, converted to $H_0 = 75$.

[c] Morphological types as used by Jansen et al. 2000b, except that we refer to all lenticular galaxies from L− to S0/a as "S0."

[d] Vader & Vigroux 1991 observe possible spiral arms in their continuum-subtracted *B*-band image of this galaxy.

TABLE 2

POSITION ANGLES OBSERVED

Galaxy	Major Axis P.A.[a]	Stellar RC P.A.	Gas RC PA
NGC 3011.....	52	50	52
A11332+3536.....	123	122, 32 (minor axis)	Same observations[b]
NGC 5173.....	100	100	Same observation[b]
NGC 7360.....	153	153	153
A23542+1633.....	12	20[c]	12, 102 (minor axis)

[a] Major axis P.A.'s are as compiled by Jansen et al. 2000b from the Uppsala General Catalog of Galaxies (UGC; Nilson 1973), except for NGC 5173, for which the UGC lists indefinite P.A. Vader & Vigroux 1991 measure a P.A. of 100 ± 5 from their high-quality *B*-band image of this galaxy.

[b] For A11332+3536 and NGC 5173, we do not have data in the 6000–7000 Å range, so our primary gas RC's are derived from [O III] and Hβ emission lines in the stellar absorption-line spectra.

[c] This observation was obtained at the Multiple Mirror Telescope Observatory, a facility operated jointly by the University of Arizona and the Smithsonian Institution.

TABLE 3

GAS AND STAR FORMATION PROPERTIES OF COUNTERROTATORS

Galaxy	$M_{\rm H\ I}$[a] ($M_\odot$)	$M_{\rm H\ I}/L_B$ ($M_\odot/L_\odot$)	SFR[b] ($M_\odot$ yr^{-1})	T[c] (Gyr)	EW(Hα)[d] (Å)	$B-R$[e] (mag)
NGC 3011.....	8.6E+07	0.07	0.055	1.6	−15.81	1.20
A11332+3536.....	2.4E+08	0.12	0.096	2.5	−15.42	1.17
NGC 5173.....	2.1E+09	0.28	0.078	27	−3.13	1.29
NGC 7360.....	3.6E+09	0.39	0.073	49	−2.37	1.35
A23542+1633.....	2.3E+09	1.21	0.220	11	−62.33	0.69

[a] Computed from H I fluxes (Bottinelli et al. 1990; Theureau et al. 1998).
[b] Computed from Hα fluxes (R. Jansen, private communication) using the calibration of Kennicutt 1998.
[c] Gas consumption timescale uncorrected for recycling.
[d] Jansen et al. 2000a.
[e] Jansen et al. 2000b.

minor axis RC (Fig. 3), but these shifts do not dominate the major axis kinematics.

In the S0 A11332+3536, the apparent counterrotation may be caused by an inclined gas disk. Consistent with a misaligned disk, the minor axis gas shows velocity amplitude comparable to the major axis gas, and while the minor axis gas appears to rotate faster than the stars, the major axis gas appears to rotate slower than the stars (see Figs. 2 and 3). This galaxy also has a small bar along its minor axis. Bettoni (1989) and Galletta (1996) point out that radial motions along a bar may sometimes create a false impression of counterrotation in one-dimensional data; however, in this case the orientation of the bar makes confusion due to noncircular motions unlikely.

In NGC 3011, the stellar rotation pattern changes with radius. Stars within $\sim$0.5 kpc rotate very slowly (if at all) in the same sense as the gas, while stars at larger radii counterrotate with 3 σ confidence. This combination suggests that the inner stars may consist of two oppositely rotating stellar populations, one population having formed more recently from infalling gas. Further data would be required to test this hypothesis.

3.2. *Statistics*

Figure 1 shows the distribution of gas-stellar counterrotators in morphology and luminosity, within the context of our 67 galaxy sample as well as the larger NFGS. The bulk counterrotation frequency for the 67 galaxy sample is $\sim$7%. However, this number includes E/S0's, early-type spirals, and later type galaxies in differing proportions (§ 2.1) and would likely be lower in a properly weighted sample.

TABLE 4

NEIGHBORS OF COUNTERROTATORS[a]

Galaxy	Nearest Neighbor	Nearest Brighter Neighbor
NGC 3011.....	270 kpc, 0.6 mag fainter	440 kpc, 2 mag brighter
A11332+3536.....	175 kpc, 0.5 mag fainter	240 kpc, 0.4 mag brighter
NGC 5173.....	50 kpc, 1.2 mag fainter	180 kpc, 0.3 mag brighter
NGC 7360.....	None in UZC[b]	
A23542+1633.....	480 kpc, 0.1 mag brighter[c]	Same as nearest neighbor

[a] Based on a search of the Updated Zwicky Catalog (Falco et al. 1999) within 600 kpc and 600 km s^{-1}; all neighbors listed have $\Delta v < 250$ km s^{-1}.
[b] Small projected neighbor appears to be a background galaxy.
[c] A bright knot within this galaxy has at times been interpreted as a neighbor but is in fact part of the main galaxy.

For E/S0's taken alone, gas-stellar counterrotators comprise four of 17 emission-line galaxies in the NFGS, which we survey completely. This result yields a frequency of 24^{+8}_{-6}% (errors are 68% confidence limits from binomial distribution statistics). If we exclude the three S0's that show almost no rotation (§ 2.3), then the statistics are four in 14, or 29^{+10}_{-8}%. In sharp contrast, we find no clear cases of counterrotation among 38 Sa–Sbc spirals, although one Sa does show another form of kinematic decoupling (NGC 4795; see footnote 1). This rate of nondetection implies that, at 95% confidence, no more than 8% of such early type spirals are bulk counterrotators. For types Sc and later, we can make no statistical conclusions due to inadequate sampling.

The strong clustering of the NFGS counterrotators in the early-type morphology region of Figure 1 probably arises from two factors. First, if counterrotation originates from galaxy mergers (as discussed in § 3.3), then early-type morphologies are a natural corollary. Second, if galaxies of all types were to accrete retrograde gas with equal probability, then this gas would survive longer in relatively gas-poor early-type galaxies, where collisions with existing gas and loss of angular momentum are less important.

Figure 1 also illustrates the tendency of our gas-stellar counterrotators to have low luminosity (sub-L_*). This result may simply reflect the fact that low-luminosity galaxies, especially early types, are more likely to be gas rich, while brighter galaxies often have too little gas for us to detect, and so are not part of our sample.

Previous studies of gas-stellar counterrotation have focused on samples restricted by morphology. Jore (1997) and Haynes et al. (2000) analyze the detailed kinematics of a sample of 23 isolated, unbarred Sa galaxies. Their sample contains four bulk gas-stellar counterrotators, suggesting that we should see about one to two examples among our eight Sa's. In fact, we see none, but our results are consistent within the small number statistics. Also, we do find one Sa with kinematically decoupled gas (NGC 4795; see footnote 1), apparently nonrotating even at radii $\sim$3 kpc. The sense of gas rotation in the central $\sim$1 kpc of this galaxy is not well determined.

In two surveys of S0's with extended gas emission, Bertola et al. (1992) and Kuijken et al. (1996) independently obtain gas-stellar counterrotation frequencies of $\sim$20%–25% for samples of 15 and 17 objects, respectively. Combin-

ing the two surveys yields a frequency of $\sim 24^{+6}_{-5}\%$ for a total sample of 29 galaxies, with three objects common to both samples. Both surveys were drawn from bright galaxy catalogs and contain objects in the range $M_B \sim -21$ to -18, with a median of ~ -19.

By comparison, the 14 S0's with extended gas emission in the NFGS span luminosities from $M_B = -20.9$ to -14.7, with a median of ~ -17. Only $\sim 30\%$ of these NFGS galaxies overlap the luminosity range of the two bright galaxy surveys (see also Kannappan & Fabricant 2000). Nonetheless, our gas-stellar counterrotation statistics for these 14 S0's agree with Bertola et al. (1992) and Kuijken et al. (1996) within the errors: $14^{+9}_{-6}\%$, or $18^{+12}_{-8}\%$ if we exclude the three S0's that show almost no rotation (§ 2.3).

Such agreement suggests the possibility that similar mechanisms form emission-line S0's over a wide range of physical scales—at least $M_B \sim -21$ to -17, the range within which S0 gas-stellar counterrotators have now been detected. However, we should point out that the low-luminosity "S0" population is heterogeneous and may include objects with very different formation histories. We assigned the S0 classification purely based on morphology, so it applies to all NFGS galaxies with the visual appearance of a two-part bulge + disk structure with minimal spiral structure. At low luminosities, this category reveals at least two subclasses: mostly smooth galaxies, and knotty or otherwise peculiar galaxies, typically with centers bluer than their outer parts (often labeled blue compact dwarfs). It is possible that only the smoother subclass forms a continuum with higher luminosity S0's in terms of formation history, or alternatively that the more peculiar objects are simply at an earlier stage of evolution. Our two S0 counterrotators have most in common with the smoother subclass, although A11332+3536 does have a small central bar and tiny spiral arms.

3.3. *Formation Mechanisms*

The two most plausible formation mechanisms for gas-stellar counterrotators are late-stage gas accretion and galaxy mergers (e.g., Thakar et al. 1997; Rubin 1994, and references therein). Secular evolution cannot easily explain large quantities of chemically enriched counterrotating gas (e.g., Caldwell, Kirshner, & Richstone 1986). We do not separately discuss inclined gas disks here, since they are likely to be closely related to counterrotating disks.

Late-stage gas accretion mechanisms include acquisition of a large H I cloud, transfer of gas during a close encounter, and infall of nearby gas stimulated by a flyby of another galaxy.

Assuming that the counterrotators' H I gas rotates in the same peculiar sense as their ionized gas, accretion of a single H I cloud cannot easily explain these galaxies' substantial H I gas masses ($\sim 10^8$–$10^9\ M_\odot$; Table 3). If the accreted H I cloud were similar to the high-velocity clouds found near the Milky Way, then it would have an H I mass of $\sim 10^7\ M_\odot$, at least an order of magnitude too small (Blitz et al. 1999). Note that this estimate assumes that the high-velocity clouds are Local Group objects at ~ 1 Mpc distances—if the clouds are closer to the Milky Way, then their H I masses are even smaller (Zwaan & Briggs 2000).

The likelihood of either companion gas transfer or infall triggered by a flyby encounter is harder to evaluate, especially since the responsible galaxy may have left the neighborhood or may be too faint to be included in a galaxy catalog. We can only say that we see no strong evidence in favor of this scenario. Based on a search of the Updated Zwicky Catalog (Falco et al. 1999) within 600 kpc and 600 km s^{-1} of each counterrotator, only one counterrotator has a neighbor within 150 kpc projected on the sky (NGC 5173; see Table 4). However, Knapp & Raimond (1984) have mapped this galaxy in detail in H I, and they see no evidence for H I flow from the companion. The lack of obviously interacting companions near our counterrotators is consistent with expectations based on the analogy between counterrotation and polar rings. Brocca et al. (1997) compare the local environments of ~ 50 apparent polar ring galaxies with those of a control sample, and they find no statistical difference between the two groups in the number of close neighbors of comparable luminosity within ~ 600 kpc.

Of course, the fact that four of our five counterrotators have E/S0 morphology hints that they probably exist in regions of high local galaxy density, which density calculations confirm (courtesy N. Grogin; see Fig. 4), although the environments are only moderately dense. This observation is consistent with either flyby or merger formation scenarios.

Mergers provide a simple alternative to late-stage gas accretion mechanisms. In this case the companion is gone, so no enhanced abundance of close neighbors is expected. The scale of the merger might range from satellite accretion

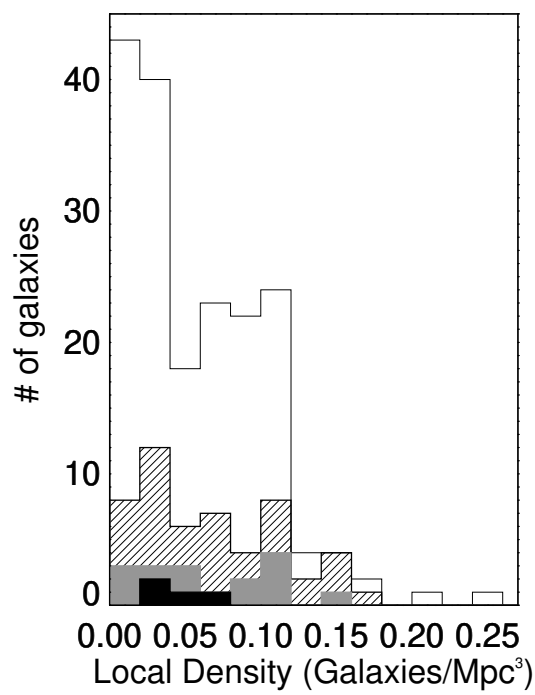

FIG. 4.—Histogram of local galaxy density around each sample galaxy. Successively smaller histograms represent in order: the entire NFGS sample, E/S0's in the NFGS sample; E/S0's with extended gas emission; and the four E/S0 gas-stellar counterrotators. Densities were provided by N. Grogin (private communication) and were derived from the CfA 2 survey using the methods described in Grogin & Geller (1998). These calculations yield densities smoothed over ~ 6.7 Mpc scales ($H_0 = 75$), counting only galaxies brighter than $M_B \sim -17$. Grogin & Geller (1998) compute densities as multiples of the mean density; we convert these to an absolute scale using their choice of mean density, 0.03 galaxies Mpc^{-3} for $H_0 = 75$. Six NFGS galaxies outside the bounds of the CfA 2 survey volume are excluded from the figure, none of which has extended gas emission.

to a major merger of comparably sized galaxies (though not necessarily comparably gas-rich). Even mergers with dwarf galaxies could easily yield the H I gas masses observed, which are similar to the H I masses of late-type dwarfs in the NFGS (computed from catalog H I fluxes; Bottinelli et al. 1990; Theureau et al. 1998).[2]

As discussed in § 3.2, the tendency for bulk counterrotators to have early-type morphologies may mean that both morphology and counterrotation have a common origin, in which case the merger would have been substantial. On the other hand, minor satellite accretion could also explain the primarily early-type morphologies of the counterrotators, if galaxies of all types accreted small neighbors, but the retrograde gas did not survive in gas-rich later types. We expect that retrograde gas will shock with existing prograde gas and either form stars immediately or lose angular momentum, creating enhanced infall and central star formation (Lovelace & Chou 1996; Kuznetsov et al. 1999).

For the round elliptical NGC 5173, either scenario is plausible. Knapp & Raimond (1984) propose that this galaxy may have formed when a gas-poor elliptical accreted a gas-rich satellite; such an event could explain the galaxy's apparently small dust-to-gas mass ratio (Vader & Vigroux 1991). Alternatively, simulations show that major mergers between gas-rich disk galaxies can also produce counterrotating gas in an elliptical (Hernquist & Barnes 1991).

For the two S0 counterrotators and the disky elliptical NGC 7360, minor mergers present a likely intermediate option. Simulations by Bekki (1998) and Naab, Burkert, & Hernquist (1999) show that minor mergers produce disky remnants, and when dissipation and star formation are included, gas-rich minor mergers can produce gas-poor S0's (Bekki 1998).

Rix, Carollo, & Freeman (1999) reject the minor merger hypothesis for low-luminosity E/S0's because observations of these galaxies show significantly greater rotational support than is seen in 3:1 disk merger simulation remnants. However, none of the simulations for which v/σ information is available include the physics of dissipation, infall, and star formation, which are clearly critical ingredients in the formation of a disk from gas rich progenitors.

In our view, minor or even gas-rich major mergers provide a very plausible formation mechanism for disky low-luminosity E/S0's, if one considers that the likely progenitors bear little resemblance to the model galaxies currently used in merger simulations. Mihos & Hernquist (1994) have shown that bulgeless disk galaxy mergers evolve very differently from bulge + disk galaxy mergers, but no one has yet modeled the complexities of a dwarf-dwarf merger. For example, the progenitors might be gas-rich dwarfs with extended filamentary H I envelopes that continue to fall into the remnant late in the merger process. The gasdynamics of small gravitational potential wells may also be important: many small early types in the NFGS display broad emission line wings, possibly related to mass outflows.

Given the steeply rising numbers of galaxies at the faint end of the galaxy luminosity function (Marzke et al. 1994), gas-rich dwarf-dwarf mergers are inevitable, and some of the remnants of such mergers may well look like S0's, or spirals embedded in S0 envelopes. The existence of very low luminosity S0's, and counterrotators as faint as $M_B \sim -17$, contrasts with the sharp decrease in early-type spirals fainter than $M_B \sim -18$ and the corresponding increase in the number of late-type dwarfs (Fig. 1; see also Sandage, Binggeli, & Tammann 1985; Schombert et al. 1995; Marzke et al. 1994). We note that the faint population of the NFGS contains a number of possible "proto-S0's"—galaxies with very blue centers and outer envelopes reminiscent of early types (Jansen et al. 2000b). These galaxies are variously typed late or early depending on the surface brightness of the envelope and the degree of inner structure. In the nomenclature of the dwarf galaxy literature, some would be known as blue compact dwarfs, a class of galaxies showing many of the expected characteristics of merger remnants (Doublier et al. 1997).[3]

Of course, some dwarf merger remnants probably just turn into bigger, brighter late-type dwarfs. For example, although the Im counterrotator A23542+1633 appears to be actively evolving, with ongoing infall (§ 3.1) and moderately strong star formation (Table 3), it does not much resemble a proto-S0 but appears more like a proto-Sd.

If the counterrotators are merger remnants, one might expect them to show signatures of enhanced past or present star formation. On the other hand, the E/S0 counterrotators' smooth morphologies (with small perturbations; see Table 1) suggest that for these four galaxies, the merger probably took place at least $\sim$1 Gyr ago (Schweizer 1998). In keeping with this view, these galaxies show moderate Hδ absorption equivalent widths ($\sim$1–3 Å; R. Jansen, private communication), consistent with starburst ages greater than $\sim$1.5 Gyr for solar metallicity (Worthey & Ottaviani 1997). By contrast, the one irregular counterrotator shows stronger Hδ absorption ($\sim$5–6 Å, subject to some uncertainty in the emission correction), suggesting a more recent/ongoing starburst. We note also that for the two faint S0's, the nominal gas consumption timescale is relatively short ($\sim$2 Gyr uncorrected for recycling; see Table 3), possibly implying rapid evolution. In fact, both of these galaxies are Markarian galaxies and have starburst nuclei (Balzano 1983).

4. CONCLUSIONS

We have searched for bulk gas-stellar counterrotation in 67 galaxies spanning a broad range of morphologies and luminosities within the $\sim$200 galaxy NFGS sample. This sample permits statistical conclusions for types E–Sbc and includes a few later types as well. However, our detections represent a lower limit to the true rate of counterrotation because the data do not permit separation of multiple kinematic components and do not rule out counterrotation beyond the radial extent of the observations.

We detect five gas-stellar counterrotators, generally of early type and low luminosity. These galaxies include two Es, two S0's, no spirals, and one Magellanic irregular. The

[2] The relative plausibility of mergers vs. gas accretion would be much better constrained for the NFGS counterrotators if we could determine the mass and extent of any counterrotating stellar populations (see comments regarding NGC 3011; § 3.1). Our existing data do not permit such an analysis, but we plan to obtain higher resolution stellar kinematic data to address this question.

[3] None of this precludes that some S0's may form through tidal stripping, but it would be rather difficult to form a counterrotator that way, unless the formation of the galaxy and the acquisition of counterrotating gas were entirely separate events.

Im galaxy counterrotates with 2.2 σ confidence and, if confirmed, represents the first known example of gas-stellar counterrotation in a Magellanic irregular. One of the S0 counterrotators probably contains an inclined gas disk rather than coplanar counterrotation; we assume that these phenomena are closely related in our interpretation.

Statistically, we conclude that 24^{+8}_{-6}% of E/S0's with extended emission are bulk gas-stellar counterrotators or 29^{+10}_{-8}% if we exclude three S0's that display very little rotation. In contrast, our nondetection of spiral counterrotators implies that no more than 8% of Sa–Sbc spirals are bulk counterrotators, at 95% confidence. This morphological dependence of counterrotation frequency may arise from two effects. First, if galaxy interactions and mergers are responsible for creating the counterrotators, then the same mechanisms will tend to produce early-type morphologies. Second, even small-scale retrograde gas accretion events that do not strongly reshape morphology will be easier to detect in E/S0's because bright spiral galaxies will typically have sufficient prograde gas to dynamically neutralize the infall.

Sa galaxies may represent a transitional case. Although we detect no Sa counterrotators, our sample is small (only eight galaxies) and includes one galaxy in which the sign of the central gas rotation is uncertain. The same galaxy shows clear gas-stellar decoupling at larger radii, where its gas displays zero apparent rotation, despite large stellar velocities. Jore (1997) finds that $\sim$15%–20% of bright, unbarred Sa's are bulk gas-stellar counterrotators.

For S0's with extended gas emission, the frequency of gas-stellar counterrotation we derive agrees with the results of Bertola et al. (1992) and Kuijken et al. (1996), although the median luminosity of our sample is $\sim$2 mag fainter ($M_B \sim -17$). The agreement suggests that similar mechanisms form this category of S0's over a wide range of physical scales, at least $-17 > M_B > -21$.

As noted by Bertola et al. (1992), every known counterrotator implies at least one corotator that formed by a similar process and probably more due to effects that tend to erase the retrograde kinematic signature. Therefore the $\sim$25% bulk counterrotation rate for emission-line E/S0's implies that at least $\sim$50% of E/S0's with extended gas emission have experienced the evolutionary processes that produce gas-stellar counterrotation.

In examining the range of possible processes, we conclude that galaxy mergers (including satellite accretion) provide the most plausible explanation for the counterrotators, especially given these galaxies' significant H I masses and lack of obvious companions. However, flyby or faint companion interactions remain a possibility. We note that the possible products of gas-rich dwarf-dwarf mergers remain largely unexplored in detailed simulations, despite clear evidence for such mergers in the faint galaxy population, and we suggest that our S0 and Im dwarf counterrotators may be products of such mergers.

Rolf Jansen generously provided his data and assisted us in using it. Norm Grogin kindly calculated local galaxy densities for us. Nelson Caldwell, Marijn Franx, and Lars Hernquist made helpful suggestions. Finally, Betsy Barton, Barbara Carter, Emilio Falco, Martha Haynes, John Huchra, Bob Kirshner, Douglas Mar, Hans-Walter Rix, and Aaron Romanowsky all provided information or resources for which we are extremely grateful. S. J. K. acknowledges support from a NASA GSRP Fellowship.

REFERENCES

Balzano, V. A. 1983, ApJ, 268, 602
Bekki, K. 1998, ApJ, 502, L133
Bertola, F., Buson, L. M., & Zeilinger, W. W. 1992, ApJ, 401, L79
Bettoni, D. 1989, AJ, 97, 79
Blitz, L., Spergel, D. N., Teuben, P. J., Hartmann, D., & Burton, W. B. 1999, ApJ, 514, 818
Bottinelli, L., Gouguenheim, L., Fouque, P., & Paturel, G. 1990, A&AS, 82, 391
Brocca, C., Bettoni, D., & Galletta, G. 1997, A&A, 326, 907
Caldwell, N., Kirshner, R. P., & Richstone, D. O. 1986, ApJ, 305, 136
Doublier, V., Comte, G., Petrosian, A., Surace, C., & Turatto, M. 1997, A&AS, 124, 405
Fabricant, D., Cheimets, P., Caldwell, N., & Geary, J. 1998, PASP, 110, 79
Falco, E. E., et al. 1999, PASP, 111, 438
Franx, M., Illingworth, G., & Heckman, T. 1989, ApJ, 344, 613
Galletta, G. 1996, in IAU Colloq. 157, Barred Galaxies, ed. R. Buta, D. A. Crocker, & B. G. Elmegreen (ASP Conf. Ser. 91; San Francisco: ASP), 429
Grogin, N. A., & Geller, M. J. 1998, ApJ, 505, 506
Haynes, M. P., Jore, K. P., Barrett, E. A., Broeils, A. H., & Murray, B. M. 2000, AJ, 120, 703
Hernquist, L., & Barnes, J. E. 1991, Nature, 354, 210
Huchra, J., Davis, M., Latham, D., & Tonry, J. 1983, ApJS, 52, 89
Hunter, D. A., Wilcots, E. M., van Woerden, H., Gallagher, J. S., & Kohle, S. 1998, ApJ, 495, L47
Jansen, R. A., Fabricant, D., Franx, M., & Caldwell, N. 2000a, ApJS, 126, 331
Jansen, R. A., Franx, M., Fabricant, D., & Caldwell, N. 2000b, ApJS, 126, 271
Jore, K. P. 1997, Ph.D. thesis, Cornell Univ.
Kannappan, S. J., & Fabricant, D. G. 2000, in ASP Conf. Ser., Galaxy Disks and Disk Galaxies, ed. J. G. Funes & E. M. Corsini (San Francisco: ASP), in press
Kannappan, S. J., Fabricant, D. G., Franx, M., Berlind, P., Balog, Z., Carter, B., Hough, L. E., Lepore, N., & Weinberg-Wolf, J. 2000, in preparation
Kennicutt, R. C., Jr. 1998, ARA&A, 36, 189
Knapp, G. R., & Raimond, E. 1984, A&A, 138, 77
Kuijken, K., Fisher, D., & Merrifield, M. R. 1996, MNRAS, 283, 543
Kurtz, M. J., Mink, D. J., Wyatt, W. F., Fabricant, D. G., Torres, G., Kriss, G. A., & Tonry, J. L. 1992, in ASP Conf. Ser. 25, Astronomical Data Analysis Software and Systems I, ed. D. M. Worrall, C. Biemesderfer, & J. V. Barnes (San Francisco: ASP), 432
Kuznetsov, O. A., Lovelace, R. V. E., Romanova, M. M., & Chechetkin, V. M. 1999, ApJ, 514, 691
Lovelace, R. V. E., & Chou, T. 1996, ApJ, 468, L25
Marzke, R. O., Huchra, J. P., & Geller, M. J. 1994, ApJ, 428, 43
Mihos, J. C., & Hernquist, L. 1994, ApJ, 431, L9
Morse, J. A., Cecil, G., Wilson, A. S., & Tsvetanov, Z. I. 1998, ApJ, 505, 159
Naab, T., Burkert, A., & Hernquist, L. 1999, ApJ, 523, L133
Nilson, P. 1973, Uppsala General Catalogue of Galaxies (Uppsala: Uppsala Astron. Obs.)
Rix, H. W., Carollo, C. M., & Freeman, K. 1999, ApJ, 513, L25
Rubin, V. C. 1994, AJ, 108, 456
Sandage, A., Binggeli, B., & Tammann, G. A. 1985, AJ, 90, 1759
Schombert, J. M., Pildis, R. A., Eder, J., & Oemler, A., J. 1995, AJ, 110, 2067
Schweizer, F. 1998, in Galaxies: Interactions and Induced Star Formation (Saas-Fee Advanced Course 26), ed. R. C. Kennicutt, Jr., et al. (Berlin: Springer), 105
Thakar, A. R., Ryden, B. S., Jore, K. P., & Broeils, A. H. 1997, ApJ, 479, 702
Theureau, G., Bottinelli, L., Coudreau Durand, N., Gouguenheim, L., Hallet, N., Loulergue, M., Paturel, G., & Teerikorpi, P. 1998, A&AS, 130, 333
Vader, J. P., & Vigroux, L. 1991, A&A, 246, 32
Whitmore, B. C., Lucas, R. A., McElroy, D. B., Steiman-Cameron, T. Y., Sackett, P. D., & Olling, R. P. 1990, AJ, 100, 1489
Worthey, G., & Ottaviani, D. L. 1997, ApJS, 111, 377
Zwaan, M. A., & Briggs, F. H. 2000, ApJ, 530, L61